Fundamental Research 1 (2021) 399–407

Contents lists available at ScienceDirect

Fundamental Research

journal homepage: http://www.keaipublishing.com/en/journals/fundamental-research/

Article

Crumpled, high-power, and safe wearable Lithium-Ion Battery enabled by nanostructured metallic textiles

Dongrui Wang[a,d], Jian Chang[a,e], Qiyao Huang[a,*], Dongdong Chen[a,f], Peng Li[a,g], Yau-Wai Denis Yu[b], Zijian Zheng[a,c,*]

[a] Laboratory for Advanced Interfacial Materials and Devices, Research Centre for Smart Wearable Technology, Institute of Textiles and Clothing, The Hong Kong Polytechnic University, Hong Kong SAR, China
[b] School of Energy and Environment, and Center of Super-Diamond and Advanced Films (COSDAF), City University of Hong Kong, Tat Chee Avenue, Hong Kong SAR, China
[c] Research Institute for Smart Energy, The Hong Kong Polytechnic University, Hong Kong SAR, China
[d] School of Chemistry and Biological Engineering, University of Science and Technology Beijing, Beijing, 100083, China
[e] Academy for Advanced Interdisciplinary Studies, Southern University of Science and Technology, Shenzhen 518055, China
[f] EPRO Advance Technology Limited, Yuen Long, Hong Kong SAR, China
[g] Institute of Microscale Optoelectronics, Shenzhen University, Shenzhen 518055, China

ARTICLE INFO

Article history:
Received 12 April 2021
Received in revised form 23 May 2021
Accepted 7 June 2021
Available online 30 June 2021

Keyword:
Energy storage
Wearable electronics
Metallic textile
Nanostructure
Flexible battery

ABSTRACT

Textile-based flexible Lithium-Ion Batteries (LIBs) show promising mechanical flexibility that is appealing for a wide variety of wearable and flexible electronic applications. The flexibility of flexible LIBs nowadays is still limited. In addition, their power performance is too low to enable high-speed charging, due to the low conductivity of the textiles. Here, we develop highly electrically conductive metallic fabrics, which are fabricated by coating nanostructured Ni or Cu (nano-reliefs) on woven cotton fabrics, as current collectors to enable crumpled, high-power, and safe wearable LIBs. The nanostructured metal coating not only effectively increases the contact area between current collectors and active materials, but also shortens the charge carrier transport paths, so that LIBs constructed on these nanostructured metallic cotton fabrics exhibit a high power density of 439 W/L and superior electrochemical stability under various mechanical deformations including folding, twisting, squeezing, and impacting. This type of nanostructured metallic textile is highly desirable for portable and wearable electronic applications.

1. Introduction

Lithium-ion batteries (LIBs) have occupied the throne of electrochemical energy storage for over 20 years, and they will continue to dominate the market for a prolonged period [1–3]. Great efforts have been devoted to seeking for better active materials to improve the energy and power densities of LIBs as a consequence of the boosting demand of electric vehicles during the past decade [4–6]. Recently, there has been a rapidly increasing interest in developing flexible LIBs that are suitable for a wide range of emerging wearable applications spanning from communication to health monitoring [7–9].

An ideal wearable LIB should be able to store or output stable electric energy in wearable deformation including bending, folding, and twisting. More importantly, it should be safe enough when the device is subject to strong impact or even sharp penetration during wearing. State-of-the-art flexible LIBs can only be bent and twisted in a relatively low degree of deformation [10]. To date, there is still an enormous gap between the requirements from wearable applications and the realistic performance of flexible LIBs.

The most urgent challenge is that existing electrode structure of flexible LIBs, in which electrode materials are coated on current collectors, is not stable enough to withstand the inevitable harsh mechanical deformations during wearing. Flexible LIBs constructed on metal foils (conventionally, aluminum (Al) for the cathode and copper (Cu) for the anode) are prone to electrode delamination or even fracture when repeatedly bent, due to the weak interfacial adhesion between active material powders and current collector, and the intrinsically poor fatigue-resistance of metals [11–14]. Recently, Zhi's group reported a type of flexible LIB using conventional Al and Cu metal foils but a novel mechanical configuration mimicking human body joints, which could withstand

* Corresponding authors.
E-mail addresses: qi-yao.huang@polyu.edu.hk (Q. Huang), tczzheng@polyu.edu.hk (Z. Zheng).

https://doi.org/10.1016/j.fmre.2021.06.007

harsh and complex deformations and were very promising for wearable applications [15]. Besides, flexible LIBs fabricated with carbon-based current collectors have been reported. Cui's group reported the flexible LIB using an ultrathin freestanding carbon nanotube (CNT) film as the current collector, which could be bent and fully charged/discharged over 20 cycles [16]. Gaikwad et al. employed a similar strategy to construct a flexible LIB with an areal capacity of 1 mAh/cm^2, and the as-made LIB could be bent into a bending radius of 10 mm [17]. Song et al. even demonstrated an origami LIB by using CNT-coated cellulose paper as current collectors, which showed a negligible loss in maximum output power over 50 cycles of folding and unfolding [18]. Three-dimensional carbon substrates have also been proposed as ideal current collectors to construct highly deformable flexible LIBs by compositing with commonly used active materials [19–21] or newly developed materials [22–25].

However, one should note that all these flexible LIBs constructed on carbon-based current collectors exhibited inferior capacity and rate capability to their counterparts using metal current collectors, which can be mainly attributed to the relatively low conductivity of carbon materials. It is known that the square sheet resistance of carbon current collectors for flexible LIBs is in the range of 1–10 Ω [16–19,22–24], which is approximately three to four orders of magnitude higher than that of a 10 μm-thick Cu foil. Moreover, such flexible LIBs with high deformability can only be realized when the carbon-based current collectors are ultrathin, leading to low mass loadings and areal capacities of active materials. Once the thickness of carbon-based current collectors is increased to a macroscopic level, the intrinsic brittle nature of carbon would result in electrode fracture when undergoing small-radius bending or folding. Therefore, the lack of an ideal current collector with low sheet resistance and high deformability lags behind the realization of wearable LIBs.

Textiles are well-known for their reliable wearability for thousands of years. The superior mechanical stability of textiles originates from the well-designed fiber-yarn-fabric hierarchical structure. Recently, nickel (Ni)-coated fabrics were introduced as conductive substrates to fabricate flexible LIBs, sodium-ion batteries, and zinc-ion batteries [26–30]. The resultant batteries showed very promising tolerance to mechanical deformation, which could smoothly input/output current during continuous folding-unfolding cycles [26]. However, the specific capacities and power densities of these batteries are low, which should be mainly ascribed to the relatively low conductivity and low surface area of Ni-coated fabrics. The specific surface area of the conductive substrates largely influences the electron transport between the current collectors and the active materials, thereby significantly affecting both energy and power densities of LIBs. To date, there is still plenty of room to improve the overall performance of wearable LIBs by rationally designing a metal-coated conductive textile as the current collector.

Herein, we demonstrate that metallic cotton fabrics coated with nanostructured Ni and Cu, in comparison to smooth coatings, are very promising for constructing high-performance wearable LIBs. Ni and Cu are typical low-cost transition metals with high electrical conductivity and good electrochemical inertness in organic electrolytes, making them highly suitable for current collectors of LIBs. We develop a wet chemistry to deposit nanostructured Ni and Cu (nano-reliefs) onto the surfaces of commercial woven cotton fabrics and apply as-fabricated metallic fabrics as current collectors for flexible LIBs. Importantly, the nanostructured metallic surface enhances the electrochemical energy storage performance by increasing the contact area between the current collector and active materials, and shortening the charge carrier transport paths. Meanwhile, the nanostructures improve the mechanical stability of the composite electrodes by increasing the interfacial adhesion between the metallic cotton fabrics and the active materials. Wearable LIBs constructed with these nanostructured metallic cotton fabrics exhibit a high power density of 439 W/L and superior electrochemical stability under various mechanical effects including folding, twisting, squeezing, and impacting, which is highly desirable for practical portable and wearable electronic applications.

2. Materials and Methods

2.1. Materials

Acetic acid, nickel sulfate hexahydrate ($NiSO_4$•$6H_2O$), nickel chloride hexahydrate ($NiCl_2$•$6H_2O$), lactic acid, boron acid (H_3BO_3), and hydrochloric acid (HCl) were purchased from Uni-Chem. Trisodium citrate ($C_6H_5Na_3O_7$), copper sulfate pentahydrate ($CuSO_4$•$5H_2O$), potassium sodium tartrate ($KNaC_4H_4O_6$•$4H_2O$), sodium hydroxide (NaOH), ethanol, and formaldehyde (37% in aqueous solution) were purchased from VWR-BDH. Potassium persulfate ($K_2S_2O_8$), Ammonium tetrachloropalladate (II) ($(NH_4)_2PdCl_4$), and dimethylamine borane were purchased from Acros. 3-(trimethoxysilyl)propyl methacrylate, [2-(methacryloyloxy)ethyl] trimethylammonium chloride (METAC, 80 wt.% in H_2O), ethylenediamine, bis(trifluoromethane)sulfonimide lithium salt (LiTFSI), lithium nitrate ($LiNO_3$), 1,3-Dioxolane (DOL), and 1,2-dimethoxyethane (DME) were purchased from Aldrich. Ammonia solution (30%) was purchased from International Lab. Active materials (lithium iron phosphate ($LiFePO_4$, LFP) and lithium titanate ($Li_4Ti_5O_{12}$, LTO), carbon black, and polyvinylidene fluoride (PVDF), and N-methyl-2-pyrrolidone (NMP) were obtained from MTI. All chemicals were used without further treatment.

2.2. Preparation of Metallic Cotton Fabrics

The preparation process of smooth or nanostructured metallic cotton fabrics is illustrated in Fig. 1(a) and Fig. S1. Cotton fabrics with the areal density of ~110 g/m^2 were firstly cut into pieces with the size of 15 × 10 cm^2 and thoroughly cleaned by deionized (DI) water. Then the cotton specimens were immersed into a 100 mL mixture solution of ethanol, acetic acid, and deionized water (95/1/4, v/v/v). After adding 1 mL of 3-(trimethoxysilyl)propyl methacrylate, the mixture was placed at room temperature for 60 min. Subsequently, the silane-modified cotton fabrics were immersed into a 10% (v/v) aqueous solution of METAC to graft the polyelectrolyte brush through in-situ radical polymerization. Polymerization was carried out at 80 oC for 60 min by using potassium persulfate as the initiator. Polymer-modified fabrics were then immersed into a 5 mM aqueous solution of $(NH_4)_2PdCl_4$ for 30 min to immobilize Pd^{2+} through ion exchange. Finally, the fabrics were immersed into an electroless deposition (ELD) bath at room temperature for different time intervals to deposit Ni or Cu on top of cotton fibers. For Ni deposition, the ELD bath contained Ni_2SO_4 (40 g/L), sodium citrate (20 g/L), lactic acid (10 g/L), and dimethylamine borane (DMAB) (1 g/L). The pH of the solution was adjusted to ~ 8.0 with ammonia before deposition. To prepare nanostructured Ni, the Ni-coated cotton fabrics after 60 min of ELD were washed and transferred immediately into an electrodeposition bath consisting of $NiCl_2$ (240 g/L), boron acid (30 g/L), and ethylenediamine (90 g/L). The pH was adjusted to ~ 4.0 with HCl solution before deposition. The electrodeposition was carried out at 60 °C by using the Ni-coated cotton fabrics as the working electrode and Ni foil as the counter electrode under a constant current density of 50 mA/cm^2. For Cu deposition, the ELD bath included a mixture of $CuSO_4$•$5H_2O$ (6.5 g/L), potassium sodium tartrate (14.5 g/L), NaOH (6 g/L), and formaldehyde (9.5 mL/L). Before each step, the fabrics were thoroughly washed with DI water.

2.3. Preparation of Composite Electrodes

Slurries consisting of active materials (LFP or LTO), carbon black, and PVDF with a weight ratio of 8:1:1 in NMP were prepared. LFP-based slurries were blade-coated onto one side of the Ni-coated cotton fabrics (denoted as NiCotton), while LTO-based slurries were coated onto the

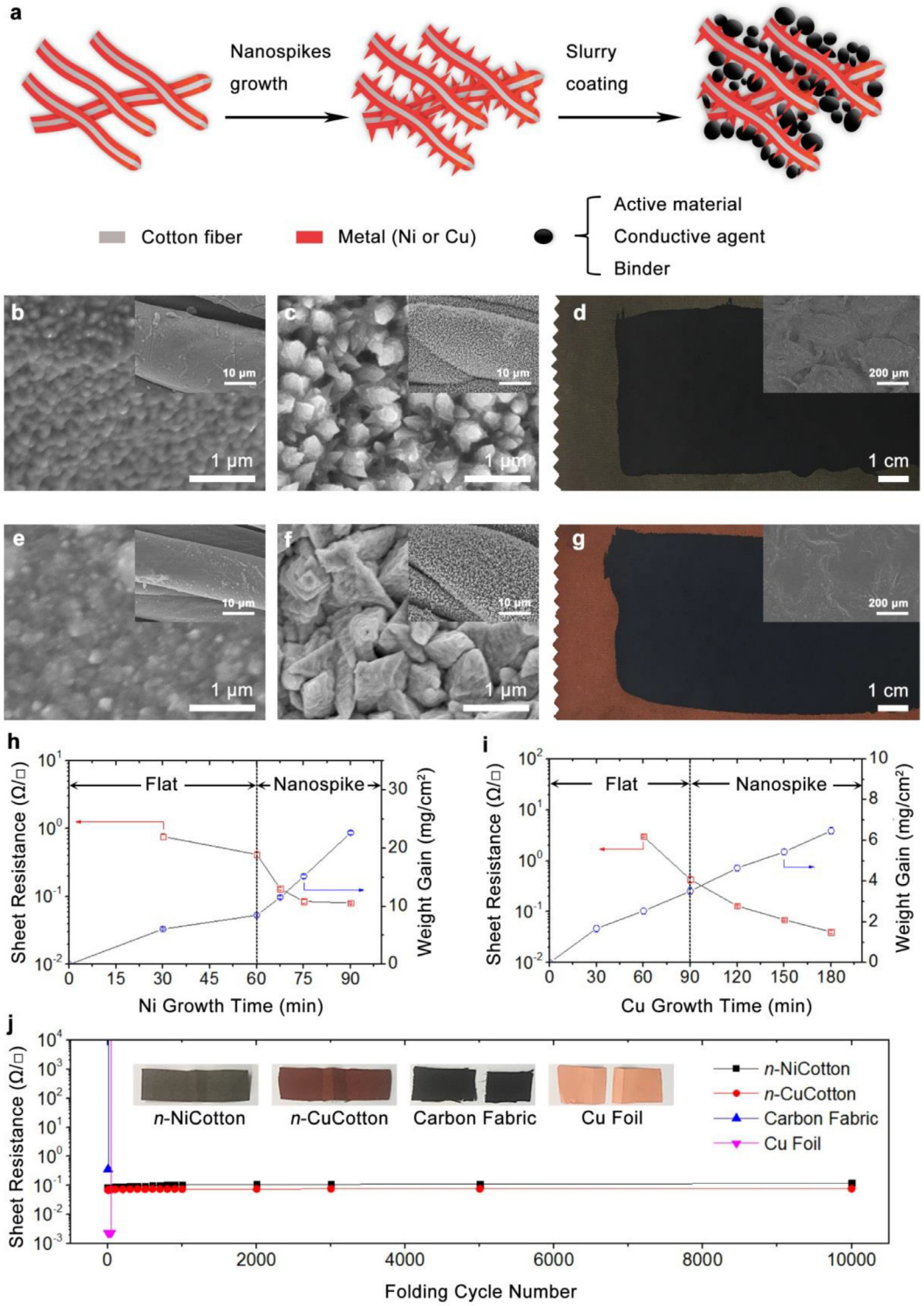

Fig. 1. (a) Schematic illustration showing the fabrication process of composite electrodes based on metallic cotton fabrics with nanostructured metal reliefs on fiber surfaces. (b) Scanning electron microscope (SEM) images of the Ni-coated cotton fabric (NiCotton) after 60 min of electroless deposition (ELD), which is denoted as *f*-NiCotton. (c) SEM images of the NiCotton fabric after 75 min of deposition of Ni (60 min of ELD and 15 min of electrodeposition), which is denoted as *n*-NiCotton. (d) Digital image of the cathode (LFP/*n*-NiCotton) prepared by blade-coating lithium iron phosphate (LFP)-based slurries on *n*-NiCotton. The inset in (d) shows the SEM image of the surface of the cathode. (e) SEM images of the Cu-coated cotton (CuCotton) fabric after 90 min of ELD, which is denoted as *f*-CuCotton. (f) SEM images of the CuCotton fabric after 150 min of deposition of Cu, which is denoted as *n*-CuCotton. (g) Digital image of the anode (LTO/*n*-NiCotton) prepared by blade-coating lithium titanate spinel (LTO)-based slurries on *n*-CuCotton. The inset in (g) shows the SEM image of the surface of the cathode. (h) Sheet resistance and areal density of NiCotton fabrics over different deposition times. (i) Sheet resistance and areal density of CuCotton fabrics with different deposition times. (j) Sheet resistance of *n*-NiCotton, *n*-CuCotton, commercial carbon fabric, and commercial Cu foil (10 μm in thickness) over 10,000 folding cycles. The insets in (j) show the digital images of the tested samples after the folding test.

Cu-coated cotton fabrics (denoted as CuCotton). The areal mass loading of LFP and LTO was limited in the range of 7–8 mg/cm^2 by tuning the gap of the blade coater. Control electrodes were also prepared by coating the slurries onto the carbon fabric (areal density = 130 g/m^2, thickness = 250 μm, sheet resistance = 0.36 Ω/□), Al foil (thickness = 16 μm), and Cu foil (thickness = 11 μm). The samples were then dried at 80 °C, punched, compressed, and completely dried under vacuum at 110 °C. The areal mass loading of active materials was carefully controlled in the range of 7.0–8.0 mg/cm^2.

2.4. Material Characterizations

The morphology and structure of the materials were observed by a scanning electron microscope (SEM) with energy-dispersive X-ray spectroscopy (EDX) (Tescan VEGA3). X-ray diffraction (XRD) curves of the samples were characterized by using a Rigaku SmartLab diffractometer. The sheet resistance of the materials was measured by using a homemade 4-probe device (Fig. S2) connected to a Keithley 2400 source meter. The tensile, peeling, and compression tests were performed by using an Instron 5565 mechanical testing machine.

2.5. Electrochemical Measurements

Stainless steel CR2032 coin cells were assembled to evaluate the electrochemical behavior of metallic fabrics and composite electrodes. The fabrics and composites electrodes were punched into round discs with a diameter of 16 mm and used as the working electrode. The Li foil with a thickness of 0.5 mm was used as the reference and counter electrodes. Pouch cells were assembled by using composite electrodes LFP/n-NiCotton (NiCotton fabric with Ni nano-reliefs) and LTO/n-CuCotton (CuCotton fabric with Cu nano-reliefs) as the cathode and the anode, respectively. The electrodes were punched into a rectangular shape of 80 mm × 46 mm. Ni tabs were connected to the metallic fabrics through welding. Aluminum laminated films with a thickness of 150 μm were used to encapsulate the pouch cells. For all the coin cells and pouch cells, 1 M LiTFSI in DOL/DME (1/1 in v/v) with 1 wt% of $LiNO_3$ was used as the electrolyte without special mention. The Celgard 2325 trilayer membrane was used as the separator. All the devices were assembled in an argon-filled glove box with oxygen < 1 ppm and moisture < 0.1 ppm.

Cyclic voltammetry tests were carried out by using a CHI 660E electrochemical workstation at room temperature. Galvanostatic charging/discharging cycles were performed by using Arbin BT2000 or Neware BTS 3000 multichannel battery testing system at various current densities. For the half cells, the C rate was determined based on the theoretical capacity of LFP (170 mAh/g) and LTO (175 mAh/g), respectively. For the full cells, the C rate was calculated based on the theoretical capacity of LFP.

3. Results

3.1. Fabrication and Characterization of the Metallic Cotton Fabrics

To convert insulating cotton fabrics into electrically conductive ones, metals were deposited onto the surface through a wet-chemistry strategy. Ni and Cu were selected as the target metals for the cathode and the anode of wearable LIBs, respectively, by taking their high conductivity, easily scalable fabrication, and low cost into account (Fig. 1(a)). We have developed a scalable approach to fabricate nanostructured NiCotton and CuCotton fabrics. The metallic fabrics in the size of 15 cm × 10 cm were prepared through polymer-assisted metal deposition (PAMD) [31,32]. As shown in Fig. S1, polyelectrolyte brushes with quaternary ammonium side groups were firstly grafted from the surface of cotton fiber and then anchored Pd^{2+} through ion exchange. Subsequently, the modified cotton fabrics were immersed in different solutions to plate Ni or Cu through Pd-catalyzed ELD at room temperature. CuCotton fabrics with Cu nanospike structures were obtained by controlling the ELD time. To prepare the nanostructured Ni, the cotton fabric after 60 min of ELD was transferred into an electrodeposition bath and further plated Ni under direct current at 60 °C. Spiky Ni in the range of several hundred nanometers was formed due to the appearance of the coordination agent ethylenediamine [33,34].

The surface morphology, areal density, and electrical conductivity of the metallic cotton fabrics over different deposition times were monitored. The SEM images show the morphology evolution of Ni and Cu on cotton fabrics (Fig. 1(b-g), Fig. S3-4). Fig. 1(h) and 1(i) demonstrate that the sheet resistance of resultant metallic fabrics decreased rapidly to lower than 10^{-1} Ω/□ as the deposition time lengthened. After 60 min of ELD, a Ni layer showing a relatively flat surface was uniformly formed on the surface of the cotton fibers (Fig. 1(b) and S3(a)). This type of NiCotton fabric with the sheet resistance of 0.42 Ω/□ is denoted as *f*-NiCotton for further investigation. Spiky Ni was successfully grown from the surface of *f*-NiCotton through additional electrodeposition (Fig. 1(c) and Fig. S3(b-d)). The morphology and thickness of the spiky Ni are greatly influenced by the plating time. Over electroplating could form a thick Ni layer of several tens of micrometers, leading to the loss of textile fibrous structure (Fig. S3(d)). 15 min electroplating yielded uniform Ni nanospikes with roots of several hundreds of nanometers (Fig. 1(c)). This NiCotton fabric, showing a sheet resistance as low as 0.085 Ω/□, is denoted as *n*-NiCotton (Fig. 1(h)).

CuCotton fabrics with similar spiky Cu morphology were prepared through one-step ELD. After 90 min of Cu ELD, a relatively flat Cu layer without the spike structure was obtained (*f*-CuCotton, Fig. 1(e), Fig. S4(a)). At this moment the sheet resistance reached 0.43 Ω/□. During 90–180 min of ELD, Cu nanospikes formed, as confirmed by the SEM observation. For CuCotton after 150 min of ELD, the nanospikes up to several hundred nanometers evenly covered all the fiber surfaces (Fig. 1(f)) and the resultant metallic fabric reached a sheet resistance of 0.07 Ω/□. This metallic fabric is denoted as *n*-CuCotton and was selected as the current collector for anodes. Further electroless deposition resulted in subtler Cu structures grown from the surface of nanospikes (Fig. S4(c)).

The surface element and crystalline structure of *n*-NiCotton and *n*-CuCotton were studied with EDX and XRD. The EDX analysis (Fig. S5) reveals the full coverage of metal on cotton fibres.XRD patterns of *n*-NiCotton and *n*-CuCotton (Fig. S6) exhibit characteristic peaks corresponding to (111), (200), and (220) planes, indicating that the Ni and Cu coating on the cotton fibers were in the face-centered cubic (fcc) structure. No diffraction peaks for any other phases or metal oxides were detected, revealing the high purity of the resultant Ni and Cu nanospikes.

Different from commercial Al and Cu foils, *n*-NiCotton and *n*-CuCotton fabrics possess great tolerance to mechanical deformations. These metallic cotton fabrics could withstand folding (bending to 180° with a curvature radius of ca. 0.2 mm) at least 10,000 times without largely deteriorating their electrical conductivity (Fig. S7). The sheet resistance of *n*-NiCotton increased from 0.085 Ω/□ to 0.12 Ω/□, and that of *n*-CuCotton increased from 0.07 Ω/□ to 0.078 Ω/□, after 10,000 folding cycles (Fig. 1(j)). These sheet resistance values are 30–50 times higher than that of the Cu foil (2.4 mΩ/□) but are far below that of the commercial carbon fabric (0.36 Ω/□). More importantly, the sheet resistance of the metallic fabrics remained at a fairly low level during folding, while the Cu foil and carbon fabric fractured and lost their conductivity after only several tens of folding. Tensile tests also confirmed that these metallic cotton fabrics possessed much larger strain and stress at break than carbon cloth and metal foils (Fig. S8). The robustness of such metallic cotton fabrics arises from the hollow structure of cotton fiber and the interlocking interface between the deposited metal layer and the grafted polyelectrolyte brushes, as we demonstrated previously [35,36]. Considering that wearable LIBs would inevitably face harsh mechanical deformations in daily applications, the nanostructured metallic

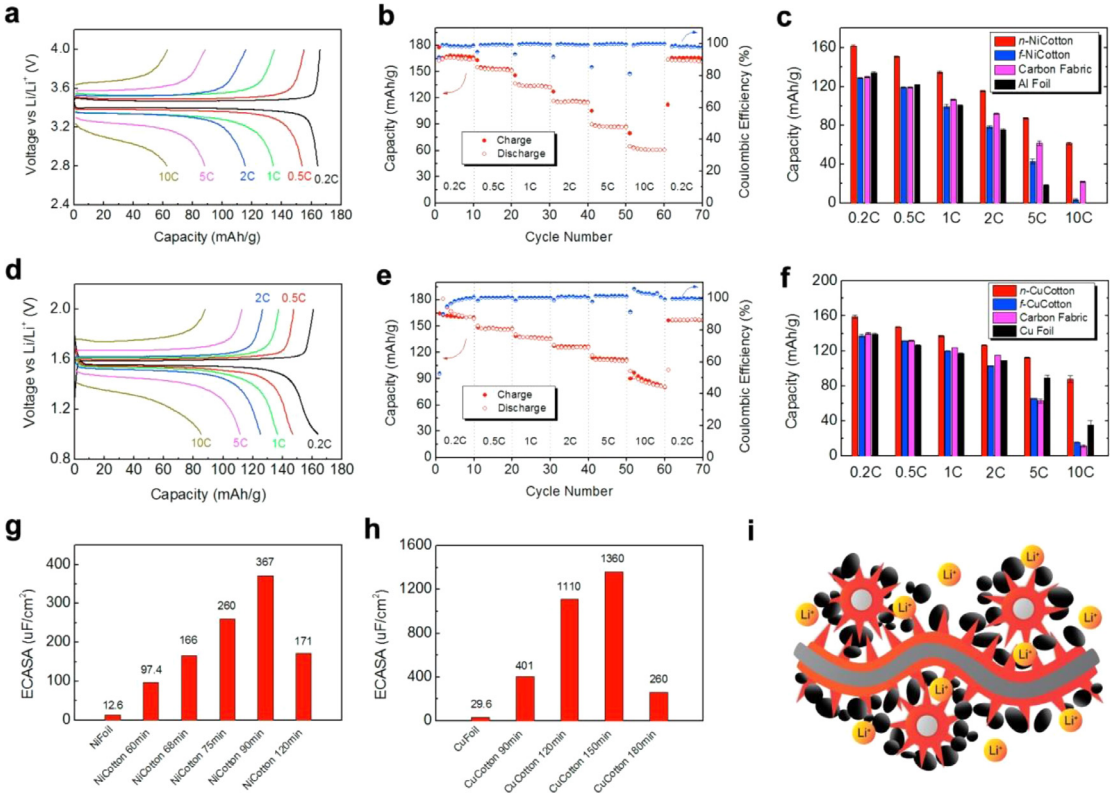

Fig. 2. (a) Typical charging/discharging voltage profiles of the LFP/n-NiCotton–based half cell within the potential window of 2.8–4.0 V under different C rates (1C = 170 mA/g of LFP). (b) Rate capability of the LFP/n-NiCotton–based half cell at various rates from 0.2 to 10 C. (c) Comparison of specific capacity of LFP using the four different current collectors under various C rates. (d) Typical charging/discharging voltage profiles of the LTO/n-CuCotton–based half cell within the potential range of 1.0–2.0 V under different C rates (1C = 175 mA/g of LTO). (e) Rate performance of the LTO/n-CuCotton half cell at various rates from 0.2 to 10 C. (f) Summary of specific capacity of LTO on different current collectors at various rates. (g) Areal electrochemical double-layer capacitance of NiCotton fabrics after different time intervals of metal chemical deposition. (h) Areal electrochemical double-layer capacitance of CuCotton after different time intervals of metal chemical deposition. (i) Schematic illustration showing the hierarchical architecture of the metallic cotton fabric with nanostructured metal reliefs on the fiber surface.

textiles are more competitive to construct wearable LIBs compared with conventional metal foils and carbon cloth.

3.2. Electrochemical Performance of Metallic Fabric-based Half Cells

Herein, LFP and LTO, which have been well investigated as active materials and widely utilized in fabricating high-power LIBs, are selected as model active materials for cathode and anode, respectively. Electrodes using NiCotton and CuCotton as current collectors were prepared through the same approach as the commercial scalable preparation, i.e., slurry preparation, blade coating, drying, cutting, pressing, and weighting. As shown in Fig. 1(d) and 1(g), the active materials are evenly dispersed on the top surface of metallic fabrics and smooth the three-dimensional reliefs of the woven structure.

Before assembling the cells, the electrochemical stability under high potentials of the NiCotton was examined. Unfortunately, we found the *n*-NiCotton could not tolerate 1 M lithium hexafluorophosphate ($LiPF_6$) solution, which is the most common electrolyte for LIBs. Cyclic voltammetry results reveal that a gradually increased polarized current was generated at the high voltage side (Fig. S9(a)), which should be ascribed to corrosion of Ni by HF in the electrolyte solution [37,38]. In comparison, the polarized current of *n*-NiCotton in 1 M LiTFSI solution decreased as the cycling (Fig. S9(b)), suggesting the corrosion of Ni was effectively eliminated. The voltage profiles of *n*-NiCotton and *n*-CuCotton under a constant charging/discharging current of 10 mA/cm^2 also prove that the chemically deposited Ni and Cu are electrochemically stable in the LiTFSI-based electrolyte solution for at least 1,000 cycles (Fig. S10). Thus the LiTFSI-based electrolyte was employed to prepare the half and full cells in the following sections.

Fig. 2(a) and 2(b) exhibit the charging/discharging voltage profiles and the rate capability of LFP/*n*-NiCotton cathode with a mass loading of 7.3 mg/cm^2 taken over various C rates ranging from 0.2 to 10 C. The specific capacity of LFP reached 161.9 mAh/g at 0.2 C, which was very close to its theoretical value of 170 mAh/g. In addition, this composite cathode showed good rate performance. The specific capacity of LFP remained at 134.5 mAh/g at 1 C. Even at a high rate of 10 C, the electrode still preserved a capacity of 61.5 mAh/g. The energy storage capacities of LFP on other current collectors including Al foil, carbon fabric, and *f*-NiCotton were also measured (Fig. 2(c), Fig. S11). For LFP/Al and LFP/*f*-NiCotton, the specific capacity was about 130 mAh/g at a low current density of 0.2 C and was nearly zero under a high C rate of 10. The LFP/carbon fabric showed better capacity at high current densities, which remained at 21.9 mAh/g at 10 C. When comparing the specific capacities of LFP coating on *n*-NiCotton to those on the Al foil, carbon fabric, and *f*-NiCotton, the LFP/*n*-NiCotton electrode shows much better energy storage capability at all tested C rates (Fig. 2(c)). The improved capacity should be attributed to the high conductivity and the high surface area of *n*-NiCotton.

For the LTO half cells, the galvanostatic discharging/charging results also prove that using *n*-CuCotton as the current collector can largely improve the specific capacity of LTO under C rates from 0.2 to 10. The voltage profiles versus capacity of the various electrodes are listed in Fig. 2(d-f) and Fig. S12. For LTO electrodes coated on Cu foil, the Coulumbic efficiency under high C rates such as 5 C and 10 C is rather unstable, suggesting a poor electron transportation (Fig. S12(a-b)). By

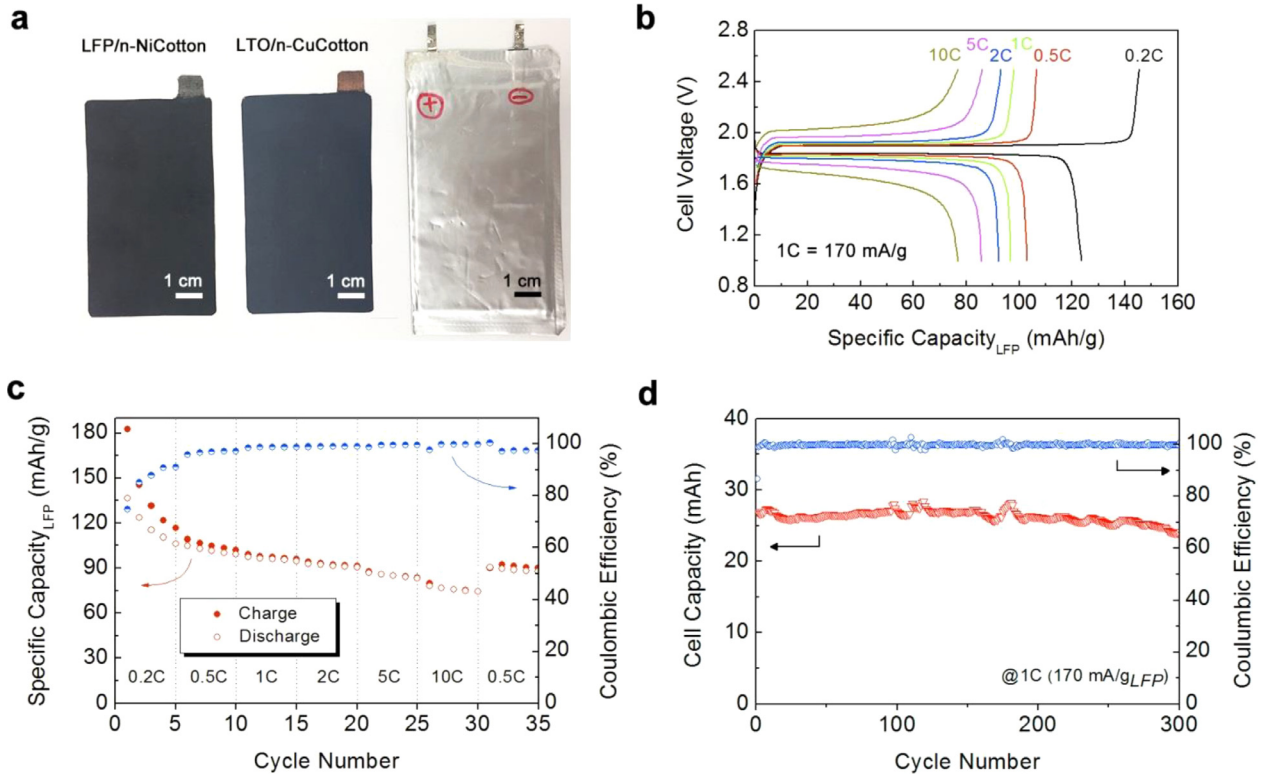

Fig. 3. (a) Digital image of the punched LFP/n-NiCotton cathode, LTO/n-CuCotton anode, and one encapsulated full cell device. (b) Typical galvanostatic charging/discharging voltage profiles of the full cell device within voltage window of 1.0–2.5 V under C rates from 0.2 C to 10 C (1C = 170 mA/g of LFP). (c) Rate capacity of the full cell. (d) Cycling performance and Coulombic efficiency of the full cell under 1 C.

using carbon fabric or *f*-CuCotton fabric as the current collector, the capacity of LTO under high C rates can be improved (Fig. S12(c-f)). The highest improvement in the capacity of LTO was obtained by using the *n*-CuCotton as the current collector. As shown in Fig. 2(f), the specific capacity of LTO at 0.2 C, 0.5 C, 1 C, 2 C, 5 C, and 10 C reaches 159.0, 147.2, 137.0, 126.6, 112.6 and 87.5 mAh/g. The areal capacities of LFP and LTO under various C rates (Fig. S13) also verify that the metallic cotton fabrics with nanostructured Ni and Cu coating are the better choices than metal foil and carbon fabrics in improving the energy storage capability of active materials, especially under high current densities.

The outstanding specific capacity and rate performance of metallic cotton fabrics with nanostructured Ni and Cu coating are greatly attributed to the Ni and Cu nano-reliefs. These nanostructures on metallic fibers can increase the effective surface area of metal, which should be beneficial to enhancing the contact of active materials with the current collectors and therefore boosting the electron transport. To verify the enhancement of the effective surface area of metal on *n*-NiCotton and *n*-CuCotton, the electrochemical active surface area (ECASA) of metallic cotton fabrics was estimated by measuring their electrochemical double-layer capacitance (Fig. S14). As shown in Fig. 2(g) and 2(h), the metallic cotton fabrics exhibit much higher areal capacitance than metal foils. The measurements yielded ECASA factors of 8, 21, 14, and 46 for *f*-NiCotton, *n*-NiCotton, *f*-CuCotton, and *n*-CuCotton when taking the flat Ni and Cu foils as the reference (Table S1), that is, the effective ECASA for Li ion transport was enhanced by about 10 folds when using the *f*-NiCotton and *f*-CuCotton to replace metal foils. The ECASA was further improved by 3 folds after introducing the nanostructured Ni or Cu reliefs. The highly improved ECASA of *n*-NiCotton and *n*-CuCotton guaranteed high interface areas between the metallic fabrics and the active materials, which offered more pathways for electron transport from active materials to the current collector, shortening the effective distance of charge carrier transport, and thereby, improving lithiation/delithiation kinetics of the composite electrodes (Fig. 2(i)).

3.3. Performance of Metallic Fabric-based Full Cells

The LFP/*n*-NiCotton and LTO/*n*-CuCotton electrodes were matched and assembled into full cells with an electrode size of 80 mm × 46 mm (Fig. 3(a)). The total thickness of obtained full battery was about 700 μm, in which the two encapsulation layers of Al laminated film cost 300 μm. Galvanostatic charging/discharging voltage profiles and rate performance of the LFP/*n*-NiCotton//LTO/*n*-CuCotton full cell are shown in Fig. 3(b) and 3(c). The battery presented stable voltage plateaus under various C rates from 0.2 to 10 C. Under a low current density of 0.2 C, the voltage plateaus for charging and discharging was 1.90 V and 1.83 V, respectively. The differential voltage between charging and discharging was gradually amplified to approximately 0.4 V as the current density increased from 0.2 to 10 C. The battery delivered averaged reversible capacities of 118.5, 101.7, 96.1, 91.6, 84.9, and 75.9 mAh/g (for LFP) under C rates of 0.2, 0.5, 1, 2, 5 and 10. These values were slightly lower than those achieved in LFP-based half cells, which should be mainly induced by the low Coulombic efficiencies under low current densities. It is also worthy of mentioning that the Coulombic efficiency of the full battery at the first cycle under 0.2 C was only 74.7%. Such low-efficiency values should be mainly ascribed to the irreversible electrochemical reactions of *n*-NiCotton with electrolytes under high voltages (Fig. S9(b) and Fig. S10(a)), which are more noticeable at low charging/discharging rates. When the current density went back down to 0.5 C from 10 C, the battery resumed the specific capacity to 90.3 mAh/g, revealing relatively good stability.

Fig. 3(d) gives the cycling performance of one full cell device under 1 C. The discharged capacity decayed from its initial value of 27.0 mAh to 23.9 mAh after 300 cycles and further dropped to 18.5 mAh after 500 cycles. The capacity retention of the full cell under 1 C was therefore 88.5% at 300 cycles and 68.5% at 500 cycles. The initial areal capacity of the battery was calculated to be 0.734 mAh/cm^2, corresponding to

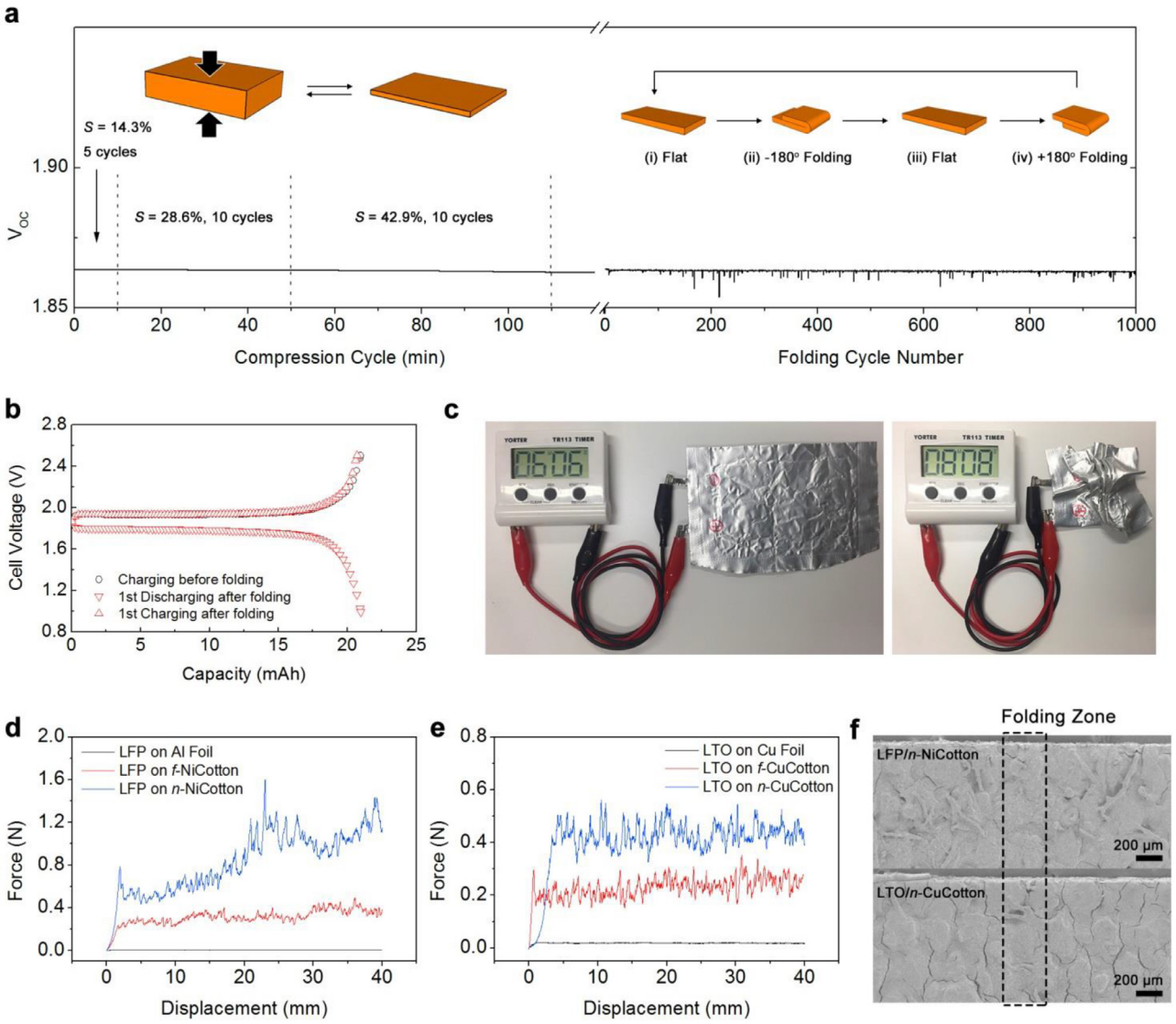

Fig. 4. (a) Left: Real-time open-circuit voltage (VOC) of one full cell device under the application of the compresstion strain of 14.3%, 28.6%, and 42.9%. Right: Real-time VOC of one full cell during 1,000 mechanical folding cycles with a frequency of ~0.2 Hz. The insets in (a) show the steps in one compression cycle (left) and one folding cycle (right). (b) Charging and discharging curves of the full cell before and after 1,000 folding cycles. (c) Digital images of one full cell in its flat and crumpled stages. (d) Adhesion force curves of LFP electrodes on Al foil, f-NiCotton, and n-NiCotton fabrics. (e) Adhesion force curves of LTO electrodes on Cu foil, f-CuCotton, and n-CuCotton fabrics. (f) SEM image showing the folding zone of the LFP/n-NiCotton cathode and LTO/n-CuCotton anode.

a specific capacity of 97.9 mAh/g (for LFP). This value dropped to ca. 11.5 mAh/g when the capacity was divided by the total mass of cathode (35.9 mg/cm^2), anode (26.5 mg/cm^2), and separator (1.25 mg/cm^2). The Ragone plot of the obtained full cell is shown in Fig. S15. The metallic cotton fabric-based full battery could deliver an energy density of 21 Wh/L under a power density of 439 W/L. Taking into consideration the volume occupied by Al-plastic encapsulation film , the energy density and the power density dropped to 12 Wh/L and 251 W/L, respectively. The relatively low energy density could be easily enhanced by utilizing more energetic active material pairs such as LFP/graphite, or by the double-sided coating of active materials on the metallic fabric and stacking multilayers of the electrodes.

More importantly, the as-fabricated metallic cotton fabric-based full battery presents superior stability when undergoing mechanical deformations. We monitored the open-circuit voltage (V_{OC}) of the LFP/*n*-NiCotton//LTO/*n*-CuCotton full cell under compression and folding. As shown in Fig. 4(a), the full cell could deform reversibly in the thickness direction when applying a compression strain as high as 42.9%. The change in V_{OC} was quite small when lower strains of 14.3% and 28.6% were applied. At the same time, the V_{OC} only dropped ~1 mV during the 10 cycles of 42.9% of compression strain. We also tested the V_{OC} of the full cell under folding-unfolding cycles. As shown in Fig. 4(a), the folding and unfolding operations to the full cell could only cause a V_{OC} fluctuation within 10 mV. The charging voltage profiles before and after 1,000 folding cycles are nearly the same (Fig. 4(b)), indicating that mechanical folding had little influence on the electrochemical performance of the full cell. To demonstrate the robustness of the metallic cotton fabric-based full battery, we used a fully charged metallic cotton fabric-based battery to power a time monitor. When harsh mechanical deformations including arbitrary folding, squeezing, even heavily compacting with a hammer were applied, the device could stably output the stored electrochemical energy (Fig. 4(c), Video S1-S2). The V_{OC} of the battery during folding and squeezing was monitored by using a voltmeter (Video S3). It can be observed that the V_{OC} was stabilized at 1.858 V all the time, proving this kind of battery could work well as stable energy provisions under daily wearing conditions. The flexible battery can also be easily integrated into wearable forms via utilizing textile technologies. Video S4 shows that the encapsulated LIBs with metallic fabrics as current col-

lectors could be sewn onto a T-shirt and steadily light up 25 LEDs under various mechanical impacts.

4. Discussion

Current collectors are an indispensable part of any form of LIBs. Therefore, developing current collectors with high electrical conductivity and high mechanical stability will largely contribute to the electrochemical performance and flexibility of the relevant LIBs. The metallic cotton fabrics utilized in this work are great candidates for such types of current collectors. Firstly, the hierarchical structure of the cotton fabric, including the particular hollow tube structure of natural cotton fiber and the twisting and woven structure of cotton yarns, endows the substrate with high strength and high tolerance to external tensile/compressive/twisting strains. Secondly, the strong chemical bonding of the metal layer on the cotton fiber surface inherits the great mechanical stability of the textile structure. It should be mentioned that Ni and Cu coating layers were prepared through a polymer-assisted metal process. The high density of hydroxyl groups on cotton cellulose fibers enables the efficient grafting of polyelectrolyte brushes and subsequently triggers high-concentrated Pd-catalyzed ELD. The interlock structure through the polyelectrolyte brush combines the chemically derived metal nanoparticles strongly onto the cotton fibers. Thirdly, the thickness and surface morphology of the Ni and Cu coating layers can be well-tuned to balance the contradiction between high electrical conductivity and low fatigue strength of metallic materials. In this work, the ELD layer of Ni and Cu was controlled to be ca. 400-600 nm. Such uniform and thin metal layers provide, simultaneously, low sheet resistance and high tolerance to mechanical folding. Moreover, the nanostructure of Ni and Cu further increases the effective surface area of metal, which should be beneficial to enhancing the contact of active materials with the current collector, therefore boosting the electron transport and material adhesion.

To further identify the effect of nanostructured metal on the adhesion of active materials, the peeling strength of LFP and LTO electrodes away from various current collectors was investigated by pulling off an adhesive tape at 180° under a constant rate of 10 mm/min (Fig. S16). As shown in Fig. 5(d), the adhesion force of the LFP-based electrode was dramatically improved from ~0.004 N (Fig. S17) to ~0.3 N by alternating the Al foil with *f*-NiCotton fabric. This value was further increased to ~0.6 N by utilizing the *n*-NiCotton as the current collector. This trend is consistent with the situations in LTO-based electrodes (Fig. 5(e)). The adhesion force of LTO on the Cu foil, *f*-CuCotton fabric, and *n*-CuCotton fabric was about 0.02 N, 0.2 N, and 0.4 N, respectively. It should also be noted that metallic fabrics can efficiently prevent the peeling off of active materials. After adhesion force tests, most of the active materials remained on the metallic cotton fabrics (Fig. S16). In contrast, all the active materials were transferred onto the adhesive tape in the cases of using metal foils as current collectors. These observations confirm the nanostructured metal on the cotton fabrics largely increases the adhesion behaviors between the electrode layer and the current collector, providing improved structural stability to mechanical deformations for the flexible LIBs based on *n*-NiCotton and *n*-CuCotton.

5. Conclusions

In summary, nanostructured Ni and Cu-coated cotton fabrics were prepared through a scalable wet-chemistry approach and used as current collectors to construct flexible LIBs. The resultant *n*-NiCotton and *n*-CuCotton with Ni and Cu nanospikes exhibited low sheet resistance (< 0.1 Ω/□) and superior tolerance to mechanical deformations. The sheet resistance of the metallic cotton fabrics revealed nearly no change during 10,000 folding-unfolding cycles. Robust flexible LIBs were fabricated based on these *n*-NiCotton and *n*-CuCotton fabrics. The nanostructure of Ni and Cu enabled the high contact area between active materials and the fabric current collector, which improved the electrochemical kinetics and the mechanical stability of the electrodes. Thus the obtained LFP/*n*-NiCotton//LTO/*n*-CuCotton full batteries can deliver a high power density of 439 W/L. More importantly, the obtained metallic fabric-based LIBs can stably output electrochemical energy after 1000 folding cycles. Furthermore, the developed Ni/Cu-coated cotton fabrics may not be limited to the tested LFP and LTO electrodes and could be extended to other high-energy active materials such as sulfur, silicon, and lithium metal. We believe that this type of metallic cotton fabric will pave the way to the development of wearable energy storage devices.

Declaration of Competing Interest

The authors declared that they have no conflict of interest to this work.

Acknowledgments

This work was supported by the NSFC/RGC Joint Research Scheme under Research Grants Council [N_PolyU528/16] and Shenzhen Municipal Science and Technology Innovation Commission [A0030246].

Supplementary materials

Supplementary material associated with this article can be found, in the online version, at doi:10.1016/j.fmre.2021.06.007.

References

[1] J.W. Choi, D. Aurbach, Promise and reality of post-lithium-ion batteries with high energy densities, Nat. Rev. Mater. 1 (2016) 1–16.
[2] J. Liu, H. Yuan, X. Tao, et al., Recent progress on biomass-derived ecomaterials toward advanced rechargeable lithium batteries, EcoMat 2 (2020) e12019.
[3] Y. Sun, N. Liu, Y. Cui, Promises and challenges of nanomaterials for lithium-based rechargeable batteries, Nat. Energy 1 (2016) 16071.
[4] J. Chang, Q. Huang, Y. Gao, et al., Pathways of developing high-energy-density flexible lithium batteries, Adv. Mater. (2021) 2004419.
[5] A. Vlad, N. Singh, C. Galande, et al., Design considerations for unconventional electrochemical energy storage architectures, Adv. Energy Mater. 5 (2015) 1402115.
[6] D. Lin, Y. Liu, Y. Cui, Reviving the lithium metal anode for high-energy batteries, Nat. Nanotechnol. 12 (2017) 194.
[7] Q.Y. Huang, D.R. Wang, Z.J. Zheng, Textile-based electrochemical energy storage devices, Adv. Energy Mater. 6 (2016) 1600783.
[8] X. Pu, L. Li, H. Song, et al., A self-charging power unit by integration of a textile triboelectric nanogenerator and a flexible lithium-ion battery for wearable electronics, Adv. Mater. 27 (2015) 2472–2478.
[9] H. Yu, N. Li, N. Zhao, How far are we from achieving self-powered flexible health monitoring systems: an energy perspective, Adv. Energy Mater. 11 (2021) 2002646.
[10] Panasonic Corporation, Panasonic develops bendable, twistable, flexible lithium-ion battery (2016) https://news.panasonic.com/global/press/data/2016/09/en160929-8/en160929-8.html. (Accessed 8 Apr 2021).
[11] A.J. Blake, R.R. Kohlmeyer, L.F. Drummy, et al., Creasable batteries: understanding failure modes through dynamic electrochemical mechanical testing, ACS Appl. Mater. Inter. 8 (2016) 5196–5204.
[12] Z. Song, X. Wang, C. Lv, et al., Kirigami-based stretchable lithium-ion batteries, Sci. Rep. 5 (2015) 1–9.
[13] M. Park, H. Cha, Y. Lee, et al., Postpatterned electrodes for flexible node-type lithium-ion batteries, Adv. Mater. 29 (2017) 1605773.
[14] J. Chang, Q.Y. Huang, Z.J. Zheng, A figure of merit for flexible batteries, Joule 4 (2020) 1346–1349.
[15] A. Chen, X. Guo, S. Yang, et al., Human joint-inspired structural design for a bendable/foldable/stretchable/twistable battery: achieving multiple deformabilities, Energ. Environ. Sci. (2021), doi:10.1039/D1EE00480H.
[16] L. Hu, H. Wu, F.La Mantia, et al., Thin, flexible secondary li-ion paper batteries, ACS Nano 4 (2010) 5843–5848.
[17] A.M. Gaikwad, B.V. Khau, G. Davies, et al., A high areal capacity flexible lithium-ion battery with a strain-compliant design, Adv. Energy Mater. 5 (2015) 1401389.
[18] Z. Song, T. Ma, R. Tang, et al., Origami lithium-ion batteries, Nat. Commun. 5 (2014) 1–6.
[19] W. Liu, Z. Chen, G. Zhou, et al., 3d Porous sponge-inspired electrode for stretchable lithium-ion batteries, Adv. Mater. 28 (2016) 3578–3583.
[20] H. Lu, J. Hagberg, G. Lindbergh, et al., $Li_4Ti_5O_{12}$ flexible, lightweight electrodes based on cellulose nanofibrils as binder and carbon fibers as current collectors for li-ion batteries, Nano Energy 39 (2017) 140–150.
[21] Y. Zhao, J. Guo, Development of flexible Li-Ion batteries for flexible electronics, InfoMat 2 (2020) 866–878.
[22] B. Liu, J. Zhang, X. Wang, et al., Hierarchical three-dimensional $ZnCo_2O_4$ nanowire arrays/carbon cloth anodes for a novel class of high-performance flexible lithium-ion batteries, Nano Lett. 12 (2012) 3005–3011.

[23] Z. Gao, N. Song, Y. Zhang, et al., Cotton-textile-enabled, flexible lithium-ion batteries with enhanced capacity and extended lifespan, Nano Lett. 15 (2015) 8194–8203.
[24] Z. Deng, H. Jiang, Y. Hu, et al., 3D ordered macroporous MoS_2@C nanostructure for flexible Li-ion batteries, Adv. Mater. 29 (2017) 1603020.
[25] Y. Li, Y.F. Du, G.H. Sun, et al., Self-standing hard carbon anode derived from hyper-linked nanocellulose with high cycling stability for lithium-ion batteries, EcoMat 3 (2021) e12091.
[26] Y.H. Lee, J.S. Kim, J. Noh, et al., Wearable textile battery rechargeable by solar energy, Nano Lett. 13 (2013) 5753–5761.
[27] K. Dong, Y.C. Wang, J. Deng, et al., A highly stretchable and washable all-yarn-based self-charging knitting power textile composed of fiber triboelectric nanogenerators and supercapacitors, ACS Nano 11 (2017) 9490–9499.
[28] Y.h. Zhu, S. Yuan, D. Bao, et al., Decorating waste cloth via industrial wastewater for tube-type flexible and wearable sodium-ion batteries, Adv. Mater. 29 (2017) 1603719.
[29] Z.H. Guo, M. Liu, Z. Cong, et al., Stretchable textile rechargeable zn batteries enabled by a wax dyeing method, Adv. Mater. Technol. 5 (2020) 2000544.
[30] Y. Zhu, M. Yang, Q. Huang, et al., V_2O_5 textile cathodes with high capacity and stability for flexible lithium-ion batteries, Adv. Mater. 32 (2020) 1906205.
[31] P. Li, Y. Zhang, Z.J. Zheng, Polymer-assisted metal deposition (PAMD) for flexible and wearable electronics: principle, materials, printing, and devices, Adv. Mater. 31 (2019) 1902987.
[32] J. Chang, J. Shang, Y.M. Sun, et al., Flexible and stable high-energy lithium-sulfur full batteries with only 100% oversized lithium, Nat. Commun. 9 (2018) 4480.
[33] T. Hang, A. Hu, H. Ling, et al., Super-hydrophobic nickel films with micro-nano hierarchical structure prepared by electrodeposition, Appl. Surf. Sci. 256 (2010) 2400–2404.
[34] T. Hang, M. Li, Q. Fei, et al., Characterization of nickel nanocones routed by electrodeposition without any template, Nanotechnology 19 (2007) 035201.
[35] X.L. Wang, C. Yan, H. Hu, et al., Aqueous and air-compatible fabrication of high-performance conductive textiles, Chem. Asian J. 9 (2014) 2170–2177.
[36] Q.Y. Huang, D.R. Wang, H. Hu, et al., Additive functionalization and embroidery for manufacturing wearable and washable textile supercapacitors, Adv. Funct. Mater. 30 (2020) 1910541.
[37] T. Liu, L. Zhao, D. Wang, et al., Corrosion resistance of nickel foam modified with electroless Ni-P alloy as positive current collector in a lithium ion battery, RSC Adv. 3 (2013) 25648–25651.
[38] B. Guitián, X. Nóvoa, A. Pintos, Development of conversion coatings on iron via corrosion in $LiPF_6$ Solution, Electrochim. Acta 304 (2019) 428–436.

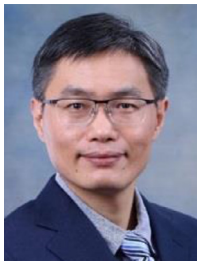

Dongrui Wang current is the Full Professor at University of Science and Technology Beijing (China). He received his B.Eng. (2003) and Ph.D. (2009) in polymer science and engineering from Tsinghua University (China). After a postdoctoral stay at the same university, he joined University of Science and Technology Beijing (China) as an Associate Professor in 2011 and was promoted to full Professor in 2016. From 2015 to 2018, he worked in Prof. Zijian Zheng's group at The Hong Kong Polytechnic University as a visiting researcher. His research interest involves electroactive soft matters, flexible materials and devices for electrochemical energy storage, and high-performance composites.

Zijian Zheng is a full professor at the Institute of Textiles and Clothing at The Hong Kong Polytechnic University. He received his B.Eng. degree (2003) in chemical engineering at Tsinghua University, Ph.D. degree (2007) in chemistry and nanoscience at the University of Cambridge, and postdoctoral training at Northwestern University between 2008 and 2009. His research interests include surface and polymer science, nanofabrication, flexible and wearable materials and devices, and energy. He is elected as Founding Member of The Young Academy of Sciences of Hong Kong.